

SCP

CERN/SPSC 98-28  
SPSC/M615  
12 October 1998

CERN LIBRARIES, GENEVA



SC00000992

su 9906

## Measurement of Atmospheric Neutrino Oscillations with a High-Density Detector

M. Aglietta<sup>a</sup>, G. Bologna<sup>a,b</sup>, M. Bonesini<sup>c</sup>, M. Calvi<sup>c</sup>,  
A. Castellina<sup>d</sup>, A. Curioni<sup>c</sup>, P. Ferrari<sup>c</sup>, W. Fulgione<sup>d</sup>,  
P.L. Ghia<sup>d</sup>, R.P. Kokoulin<sup>e</sup>, G. Mannocchi<sup>b,d</sup>, F. Murtas<sup>b</sup>,  
G.P. Murtas<sup>b</sup>, P. Negri<sup>c</sup>, M. Paganoni<sup>c</sup>, L. Periale<sup>d</sup>,  
A.A. Petrukhin<sup>e</sup>, P. Picchi<sup>b,d,a</sup>, A. Pullia<sup>c</sup>, S. Ragazzi<sup>c</sup>,  
N. Redaelli<sup>c</sup>, L. Satta<sup>b</sup>, T. Tabarelli de Fatis<sup>c</sup>, F. Terranova<sup>c</sup>,  
A. Tonazzo<sup>c</sup>, G. Trincherò<sup>d</sup>, P. Vallania<sup>d</sup>, B. Villone<sup>d</sup>

<sup>a</sup>*Dipartimento di Fisica, Università di Torino, Torino, Italy*

<sup>b</sup>*Laboratori Nazionali di Frascati, INFN, Frascati, Italy*

<sup>c</sup>*Dipartimento di Fisica, Università di Milano and INFN, Milano, Italy*

<sup>d</sup>*Istituto di Cosmogeofisica, CNR, Torino, Italy*

<sup>e</sup>*Moscow Engineering Physics Institute, Moscow, Russia*

## Abstract

We propose an experiment on atmospheric neutrinos having the capability to test the claim of Super-Kamiokande for neutrino oscillations, exploiting the high energy component of the atmospheric neutrino spectra. This experiment will compare the event rates induced by the near and far (downward and upward) atmospheric muon neutrino beams. A modulation in the ratio of these rates as a function of the  $L/E$  will be a signature of neutrino oscillation ( $\nu_\mu$  disappearance). The detector will consist of iron planes interleaved by tracking devices, either RPCs or/and limited streamer tubes. The adoption of a fully developed and tested technique will allow considerable saving of time and manpower, since no R&D is required. With a mass in excess of 30 kt and in three years of data taking, this experiment will be sensitive to  $\nu_\mu \rightarrow \nu_x$  oscillations with  $\Delta m^2 > 6 \times 10^{-5} \text{ eV}^2$  and mixing near to maximal and fully cover the region of oscillation parameters favoured by Super-Kamiokande results. Moreover, the experimental method will enable to measure  $\Delta m^2$  in the range  $10^{-4} - 5 \times 10^{-3} \text{ eV}^2$ . For  $\Delta m^2 > 3 \times 10^{-3} \text{ eV}^2$ , this experiment will also allow to establish whether the oscillation occurs into a tau or a sterile neutrino, by looking for an excess of muon-less events at high energies produced by upward-going tau neutrinos ( $\nu_\tau$  appearance).

# 1 Introduction

In a recent paper [1] the Super-Kamiokande collaboration confirms the existence of an anomaly in the atmospheric muon neutrino fluxes. The anomaly is interpreted in terms of a  $\nu_\mu \rightarrow \nu_x$  oscillation, with mixing  $\sin^2(2\Theta) > 0.82$  and mass-square difference  $5 \times 10^{-4} < \Delta m^2 < 6 \times 10^{-3}$  eV<sup>2</sup>. The non observation of a corresponding anomaly in the electron neutrino fluxes and data from reactor experiments [2] indicates that the oscillation either concerns the muon and tau neutrino or the muon and a new sterile neutrino. An indication of the same effect has been reported also by the MACRO collaboration [3]. This result, given its relevance, should be tested by an independent experiment.

It has been shown [4] that the study of the atmospheric  $\nu_\mu$  event rate as a function of the ratio  $L/E$ , between the neutrino path length and its energy, is an effective method for the detection of an atmospheric  $\nu_\mu$  deficit, if the deficit is due to oscillations. It was further shown [5, 6] how this method can be implemented and used to measure the oscillation parameters, with a massive tracking detector. In ref. [6] a method was also discussed, based on the comparison of the rates of upward to downward muon-less neutrino events, which can distinguish between oscillation into a sterile or a tau neutrino. This paper will further extend the ideas discussed in ref. [4, 5, 6].

## 2 Experimental method

Atmospheric neutrino fluxes are not in general up/down symmetric. However, the up/down asymmetry, which is mainly due to geomagnetic effects, is reduced to the percent level for neutrino energies above 1.3 GeV [7, 8]. At these energies, for  $\Delta m^2 < 10^{-2}$  eV<sup>2</sup>, downward muon neutrinos are not affected by oscillations. Thus, they may constitute a *near* reference source. Upward neutrinos are instead affected by oscillations, since the  $L/E$  ratio of their path length over the energy ranges up to  $10^4$  km/GeV. Therefore with atmospheric neutrinos one may study oscillations with a single detector and two sources: a *near* and a *far* one. The effects of oscillations are then searched comparing the  $L/E$  distribution for the upward neutrinos, which should be modulated by oscillations, with a reference distribution obtained from the downward neutrinos. For upward neutrinos the path length  $L$  is determined by their zenith angle as  $L(\theta)$ , while the reference distribution is obtained replacing the actual path length of downward neutrinos with the mirror-distance  $L'(\theta) = L(\pi - \theta)$  (see Fig. 1). The ratio  $N_{up}(L/E)/N_{down}(L'/E)$  will then correspond to the survival probability given by

$$P(L/E) = 1 - \sin^2(2\Theta) \sin^2(1.27\Delta m^2 L/E) \quad (1)$$

with  $L$  in km,  $E$  in GeV,  $\Delta m^2$  in eV<sup>2</sup>. A smearing of the modulation is introduced by the finite  $L/E$  resolution of the detector as discussed in the following sections.

We point out that results obtained by this method are not sensitive to calculations of atmospheric fluxes.

We also remark that this method does not work with neutrinos at angles near to the horizontal ( $|\cos(\theta)| < 0.07$ ), since the path lengths corresponding to a direction and its mirror-direction are of the same order.

If evidence of neutrino oscillation from the study of  $\nu_\mu$  disappearance is obtained, a method based on  $\tau$  appearance can be used to discriminate between oscillations  $\nu_\mu \rightarrow \nu_\tau$  and  $\nu_\mu \rightarrow \nu_{sterile}$ . Oscillations of  $\nu_\mu$  into  $\nu_\tau$  would in fact result in an excess of muon-less events produced by upward neutrinos with respect to muon-less downward. Due to threshold effects on  $\tau$

production this excess would be important at high energy. Oscillations into a sterile neutrino would instead result in a depletion of upward muon-less events. Discrimination between  $\nu_\mu \rightarrow \nu_\tau$  and  $\nu_\mu \rightarrow \nu_{sterile}$  is thus obtained from a study of the asymmetry of upward to downward muon-less events. Because this method works with the high energy component of atmospheric neutrinos, it becomes effective for  $\Delta m^2 > 3 \times 10^{-3} \text{ eV}^2$ .

### 3 Choice of the Detector

The outlined experimental method requires that the energy  $E$  and direction  $\theta$  of the incoming neutrino be measured in each event. The latter, in the simplest experimental approach, can be estimated from the direction of the muon produced in the  $\nu_\mu$  charged-current interaction. The estimate of the neutrino energy  $E$  requires the measurement of the energy of the muon and of the hadrons produced in the interaction. In order to make the oscillation pattern detectable, the experimental requirement is that  $L/E$  be measured with an error smaller than half of the modulation period. This translates into requirements on the energy and angular resolutions of the detector. As a general feature the resolution on  $L/E$  improves at high energies, mostly because the muon direction gives an improved estimate of the neutrino direction. Thus the ability to measure high momentum muons (in the multi-GeV range), which is rather limited in the on-going atmospheric neutrino experiments, would be particularly rewarding.

A detector with a high efficiency on  $\mu/\pi$  separation is required for an effective implementation of the method proposed, while, leaving aside oscillations involving electron neutrinos, no stringent requirement is put on electron identification and electromagnetic energy resolution.

These arguments led to consider a large mass and high-density tracking calorimeter with horizontal sampling planes as a suitable detector [6]. A mass of a few tens of kilotons is necessary to have enough neutrino interaction rate at high energies, while the high-density enables to operate the detector as a muon range-meter. This solution has been preferred with respect to a magnetised iron spectrometer for its simplicity and because the full containment of events reduces the background due to externally produced muons stopping in the detector. Both the tau appearance method and the  $L/E$  modulation method require the identification of the neutrino flight direction. For the latter method, if the interaction vertex is not identified, this requirement is very stringent and translates into a requirement for the identification of the muon flight direction with high efficiency and high purity. This can be obtained either by time of flight measurement or by a precise measurement of multiple scattering of the muon, or a combination of the two techniques. This leaves the choice of sensitive elements open for RPCs, for time-of-flight measurement, or limited streamer tubes, equipped with time recording of the anode pulse, for multiple scattering measurement. A combination of the two techniques can also be considered.

For the tau appearance method the relevant sample will be given by muon-less events of high hadronic energy. In these events the flight direction of the incoming neutrino will be identified when the event topology will allow the identification of a vertex. Ambiguous events will be discarded. The poor response of a coarse-grain digital calorimeter to electromagnetic energy will shift towards low visible energies the  $\nu_e$  CC interactions, thus reducing the background of these events in the tau-appearance sample.

In summary, when these arguments together with costs are considered, a digital tracking calorimeter with a coarse sample appears to be the best choice. The choice of streamer tubes or RPCs as sensitive elements would also save time, since they do not require R&D.

## 4 The Detector Structure

The detector which has been considered in our simulations consists in a stack of 120 horizontal iron planes 8 cm thick and  $15 \times 30$  m<sup>2</sup> surface, interleaved by planes of sensitive elements. The sensitive elements provide two coordinates with a pitch of 3 cm. Sensitive elements are housed in a 2 cm gap between the iron planes. The height of the detector is thus 12 metres. A 2 cm gap is widely sufficient to house RPCs and their read-out elements, limited streamer tubes may require wider gaps. The total mass of the detector exceeds 34 kt. The total surface of sensitive planes is 54,000 m<sup>2</sup>; the number of read-out channels is 180,000.

For a discussion on the optimisation of the detector structure the reader is referred to [6].

## 5 Detection of Atmospheric Neutrino Oscillations

As outlined in section 2, detection of oscillation of atmospheric neutrinos and measurement of their parameters will rely on two main techniques:

- disappearance of events with a high-energy muon pointing upward;
- comparison of rates upward and downward muon-less events of high energy.

While the first technique will test the hypothesis of  $\nu_\mu$  oscillations and measure  $\Delta m^2$  provided it is smaller than  $5 \times 10^{-3}$  eV<sup>2</sup>, the second one will be used to discriminate between oscillations to a sterile or a tau neutrino.

A full simulation of the experimental apparatus has been implemented. Neutrino interactions, according to the differential flux distribution predicted at the Gran Sasso, have been kindly provided by G. Battistoni and P. Lipari. Secondary particles produced in the interactions have been propagated through the detector by means of the GEANT package.

The muon energy, obtained from range with errors due to straggling and to the uncertainty on range measurement, and the muon direction, obtained by a straight line fit to the first meter of the muon track, are measured with high precision. The hadronic energy is estimated from the hit multiplicity in the calorimeter. The detector has a coarse hadronic energy resolution and essentially no capability of reconstructing the hadronic energy flow.

### 5.1 Disappearance of muon neutrinos

In the experiment simulation, since the value oscillation parameters is not known *a priori*, a unique set of event selections and a unique analysis method have been defined in order to make the oscillation pattern detectable for every possible experimental outcome.

All the events not fully contained in a fiducial volume corresponding to about 85% of the detector have been rejected, to avoid contamination from muons externally produced and stopping in the detector. Events are retained if a muon is identified with a minimum energy of 1.3 GeV and if the muon hits at least seven layers. In this analysis we have assumed that the identification of the muon neutrino direction be fully efficient, which is in the reach of the experimental layout described.

The experimental requirement that  $L/E$  be measured with an error smaller than half of the modulation period (for every possible value of  $\Delta m^2$ ) is satisfied by selecting events having an estimated relative error on  $L/E$  not exceeding 50%.

Altogether, these selections reduce the charged current interaction rate of downward going muon neutrinos to about  $7 \text{ kt}^{-1} \cdot \text{y}^{-1}$  (20% of the total rate integrated for muon neutrinos with energies above 1 GeV). The  $L/E$  resolution on the selected sample is shown in Fig.2 and compared to the  $L/E$  resolution of the Super-Kamiokande experiment [16].

We present, as examples, the  $L/E$  distributions obtained with this method for several values of  $\Delta m^2$  and  $\sin^2(2\Theta)$  (Fig. 3) and (Fig. 4). In these figures we also show the discovery potential (allowed regions of the oscillation parameters space) of the experiment after three years of exposure, as deduced from a fit to the  $L/E$  spectra of a predictive curve folded with the detector resolution.

For  $\Delta m^2$  larger than  $5 \times 10^{-3}$ , the  $L/E$  modulation can not be resolved. Still the oscillations can be identified by a deficit of upward with respect to downward events, which will result in an average ratio of 0.5 in the case of maximal mixing. Moreover, at  $\Delta m^2$  larger than a few  $10^{-2} \text{ eV}^2$ , when upward neutrinos are fully oscillated, the oscillation pattern will become detectable in the downward sample. In this limit, the role of upward and downward neutrinos can be exchanged: a mirror path length can be assigned to upward neutrinos, which can be used as a reference  $L/E$  distribution for downward neutrinos. In summary, if an up/down asymmetry is observed, but no  $L/E$  modulation is visible, either in the upward sample, or in the downward sample, the  $\Delta m^2$  can be confined in the range  $5 \times 10^{-3} - 10^{-2} \text{ eV}^2$ ; otherwise the value of  $\Delta m^2$  can be measured.

In absence of neutrino oscillations, these arguments can be used to exclude a region of oscillation parameters. The exclusion limits at 90% and 99% C.L. that this experiment will be able to set after an exposure of three years are shown in Fig. 5. A 2% systematic uncertainty in the knowledge of the up/down ratio of atmospheric neutrino fluxes has been assumed.

## 5.2 Appearance of tau neutrinos

If evidence of neutrino oscillation from the study of  $\nu_\mu$  disappearance is observed, for  $\Delta m^2 > 5 \times 10^{-3}$  there is a method to measure the  $\nu_\tau$  appearance and/or distinguish between  $\nu_\mu \rightarrow \nu_\tau$  oscillation and  $\nu_\mu \rightarrow \nu_{sterile}$  oscillation.

The method consists in measuring the up/down ratio of the high energy muon-less events, with the vertex clearly identified, as a function of the visible energy.

An event is considered to be muon-less if it does not contain non-interacting tracks longer than 1 m (equivalent to 0.9 GeV for a m.i.p.); an estimate of the visible energy is obtained from the hit multiplicity in the two views; the up/down direction is determined by the shape of the hadronic shower development.

For sake of clarity, in table 1 we give the integrated values of the neutrino CC events rates for a detector exposure of  $100 \text{ kt} \cdot \text{y}$  and  $-1 < \cos(\theta) < 0$  (upward neutrinos); in table 2 we give the same rates but for  $-1 < \cos(\theta) < -0.5$ .

From these tables it is clear that, in order to enhance the relative  $\nu_\tau$  contribution to muon-less events, one has to select candidates with high visible energy.

The  $\nu_\mu$  CC events rejection is good at high energy because of the cut of muon with energy larger than 0.9 GeV (due to the flat  $y$  distribution of the CC interaction).

The  $\nu_e$  CC events rejection is due to the characteristic feature of the detector to filter off the electro-magnetic component of the interaction. As a consequence the visible energy is only due to the residual hadronic component as in the case of neutral current events.

A very important feature of this detector that helps in reducing the uncertainty on the up/down muon-less ratio is the non isotropy of the detector. The reason is the following: the

$E_{min}(GeV)$	$\nu_\mu$	$\nu_e$	$\nu_\tau$		
			$10^{-2} eV^2$	$5 \times 10^{-3} eV^2$	$10^{-3} eV^2$
1.	3600	1581	129	118	62
3.	1471	504	129	118	62
10.	446	106	94	83	27
30.	127	21	39	31	2.5

Table 1: Neutrino + anti-neutrino integrated CC event rate for a detector exposure of 100 kt.y and  $-1 < \cos(\theta) < 0$ . For the  $\nu_\tau$  case the columns are given with rates for three values of  $\Delta m^2$  and for maximal mixing. The integrated NC event rate is about one third of the  $\nu_\mu + \nu_e$  CC event rate.

$E_{min}(GeV)$	$\nu_\mu$	$\nu_e$	$\nu_\tau$		
			$10^{-2} eV^2$	$5 \times 10^{-3} eV^2$	$10^{-3} eV^2$
1.	1595	582	53	53	43
3.	638	161	53	53	43
10.	175	25	38	39	21
30.	48	4	18	21	2.0

Table 2: Same as table 1 but for  $-1 < \cos(\theta) < -0.5$ .

horizontal events are of little use in the up/down ratio, in fact they do not oscillate enough, their hemisphere is uncertain and the  $\nu_e$  background is larger. The fact that the detector has a vertical development and a thick sampling causes the rejection of most of horizontal NC events and  $\nu_e$  CC, because their limited vertical development prevents the identification of their direction.

An extensive simulation of the detector performance has been performed to estimate the efficiency for the up/down discrimination. The analysis of the simulated data has been performed first through visual scanning to optimise the selection cuts, then in an automated way where the best selection cuts have been implemented.

In Fig. 6 we show the differential up/down ratio as a function of the number of hits in the calorimeter, for  $\Delta m^2 = 5 \times 10^{-3}$ . The two alternative hypothesis  $\nu_\mu \rightarrow \nu_\tau$  and  $\nu_\mu \rightarrow \nu_{sterile}$  are compared. In the  $\nu_\mu \rightarrow \nu_\tau$  case there is an excess of muon-less events with high visible energy from the bottom hemisphere due to the tau decay into muon-less channels ( $BR \simeq 0.8$ ) that produce neutral current like events; in the  $\nu_\mu \rightarrow \nu_{sterile}$  case there is a lack of neutral currents from the bottom hemisphere at all visible energies because the sterile neutrino does not interact via neutral currents.

For  $\Delta m^2 = 5 \times 10^{-3}$  and in three years of data taking, the two alternative hypothesis can be separated at the 90% C.L. with a rejection power of  $10^{-2}$ , corresponding to a separation of about 3 sigma. A similar separation is obtained at larger values of  $\Delta m^2$ .

## 6 Conclusions

We have demonstrated that a high density detector of 34 kt with rough sampling and good tracking capability is well suited to solve the atmospheric neutrino puzzle as stated by the Super-Kamiokande experiment. The major improvement with respect to Super-Kamiokande relies on the exploitation of the high energy component of the atmospheric muon neutrino spectrum. This reflects in a better  $L/E$  resolution in the range around  $10^3 \text{Km/GeV}$  as can be seen in the comparison shown in Fig. 2.

This experiment exploits both appearance and disappearance methods; the oscillation parameters are measured over a wide range of  $\Delta m^2$  values and for large mixing angle. In Fig. 5 is shown the exclusion area in case of no oscillations.

The detector is easily built in a short delay because it does not require R&D phases.

This experiment, completely devoted to the atmospheric neutrino study, is complementary to those designed for long base line neutrino detection [9, 10, 11, 12, 13, 14] with artificial neutrino beams. In fact, in the energy range considered here, atmospheric neutrinos are still an unexploited source of potential discovery, since they cover a wider  $L/E$  range than long baseline beams [8]. In case of negative or uncertain results from K2K [15] this experiment will play an essential role in clarifying the Super-Kamiokande result.

## 7 Costs

The costs estimates are the following. 17 GLit (14 MCHF) for 34 kt of iron sections; 13.5 GLit (11.2 MCHF) for the active elements, either RPCs or streamer tubes; 4 GLit (3.3 MCHF) for the electronics and the read out system; 5 GLit (4.2 MCHF) for HV system, gas, and facilities. The total cost will thus be 39.5 GLit or 33 MCHF.

## Acknowledgements

Most of this work was done by F. Pietropaolo.

We gratefully acknowledge P. Lipari and G. Battistoni for providing us the neutrino events, without which this work would not have been possible.

## References

- [1] The Super-Kamiokande Collaboration, Y. Fukuda et al., *Phys. Rev. Lett.* **81**, 1562-1567 (1998)
- [2] M. Apollonio et al., *Phys. Lett. B* **420**, 397-404 (1998)
- [3] M. Ambrosio et al., INFN/AE-98/13
- [4] P. Picchi and F. Pietropaolo, "Atmospheric Neutrino Oscillations Experiments", ICGF RAP. INT. 344/1997, Torino 1997, (CERN preprint SCAN-9710037).
- [5] G. Mannocchi et al., CERN/OPEN-98-004
- [6] A. Curioni et al., hep-ph/9805249



- [7] P. Lipari, T. K. Gaisser and T. Stanev, astro-ph/9803093;
- [8] G. Battistoni and P. Lipari, hep-ph/9807475
- [9] ICARUS-CERN-MI Coll., CERN/SPSLC 96-58, SPSLC/P 304, December 1996;  
J. P. Revol *et al.*, ICARUS-TM-97/01, 5 March 1997.
- [10] H. Shibamura *et al.*, LNGS-LOI 8/97, 8 September 1997.  
H. Shibuya *et al.*, CERN-SPSC-97-24, Oct 1997. Letter of intent.
- [11] Letter of Intent for Long Baseline RICH, CERN-LAA/96-01, 1 January 1996.
- [12] M. Apollonio *et al.*, *Studies for a long baseline accelerator and atmospheric neutrino oscillation experiment at Gran Sasso*, and addendum:, expression of interest to the Gran Sasso Laboratory Scientific Laboratory, unpublished.
- [13] G.C. Barbarino *et al.*, *Nucl. Phys. B* **66**, 1988 (428)
- [14] *The Minos Long Baseline Experiment at Fermilab*, Nucl.Phys.Proc.Suppl.59:297-304,1997
- [15] K2K collaboration, KEK-PREPRINT-97-266, Jan 1998, and hep-ex/9803014.
- [16] J.G. Learned, private communication.

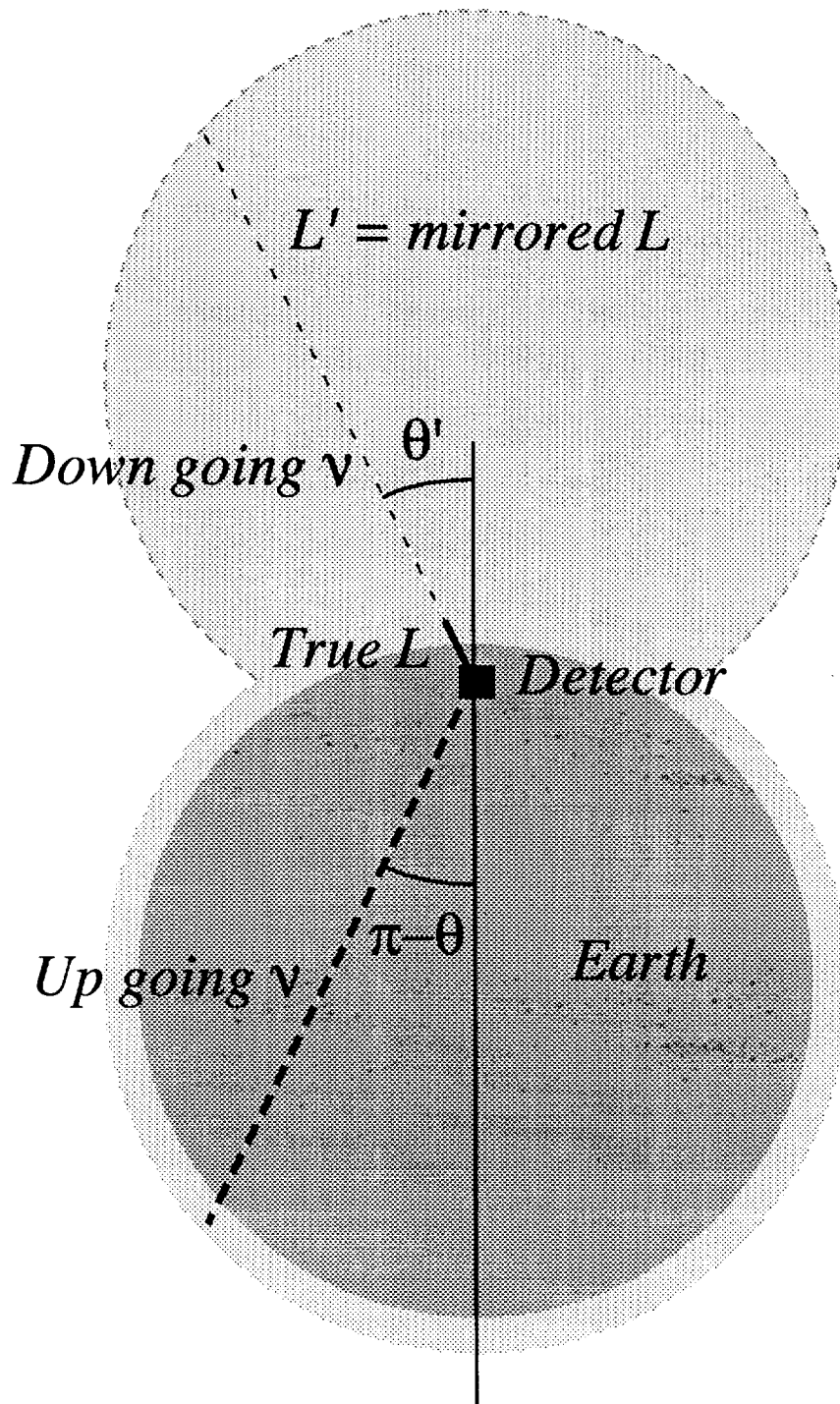


Figure 1: Artist's view of the mirror neutrino path length: downward going neutrinos (zenith angle  $\theta < \pi/2$ ) are assigned the distance they would have travelled if  $\theta = \pi - \theta$ .

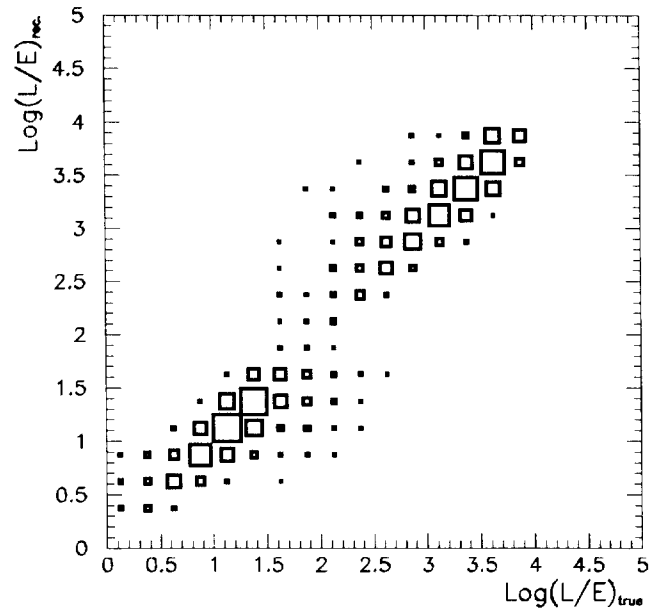
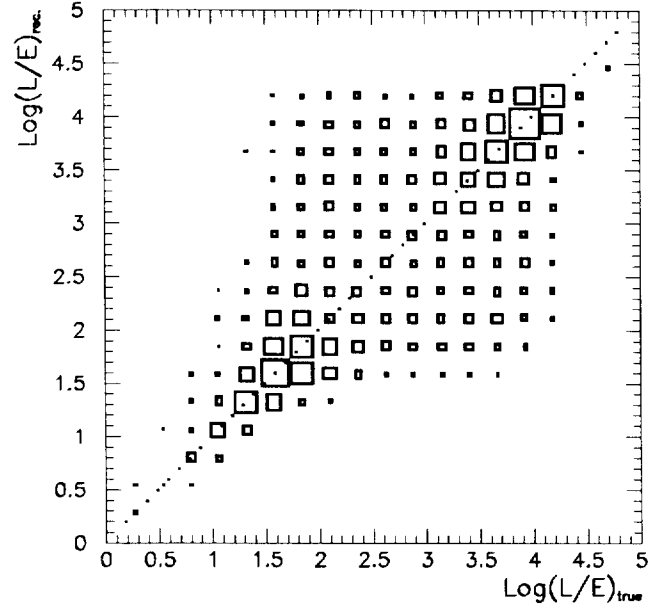


Figure 2: Reconstructed  $L/E$  versus true  $L/E$  as obtained in the simulation of our detector after the selections described in the text (bottom). For comparison the same distribution for the Super-Kamiokande experiment [16] is also shown (top).

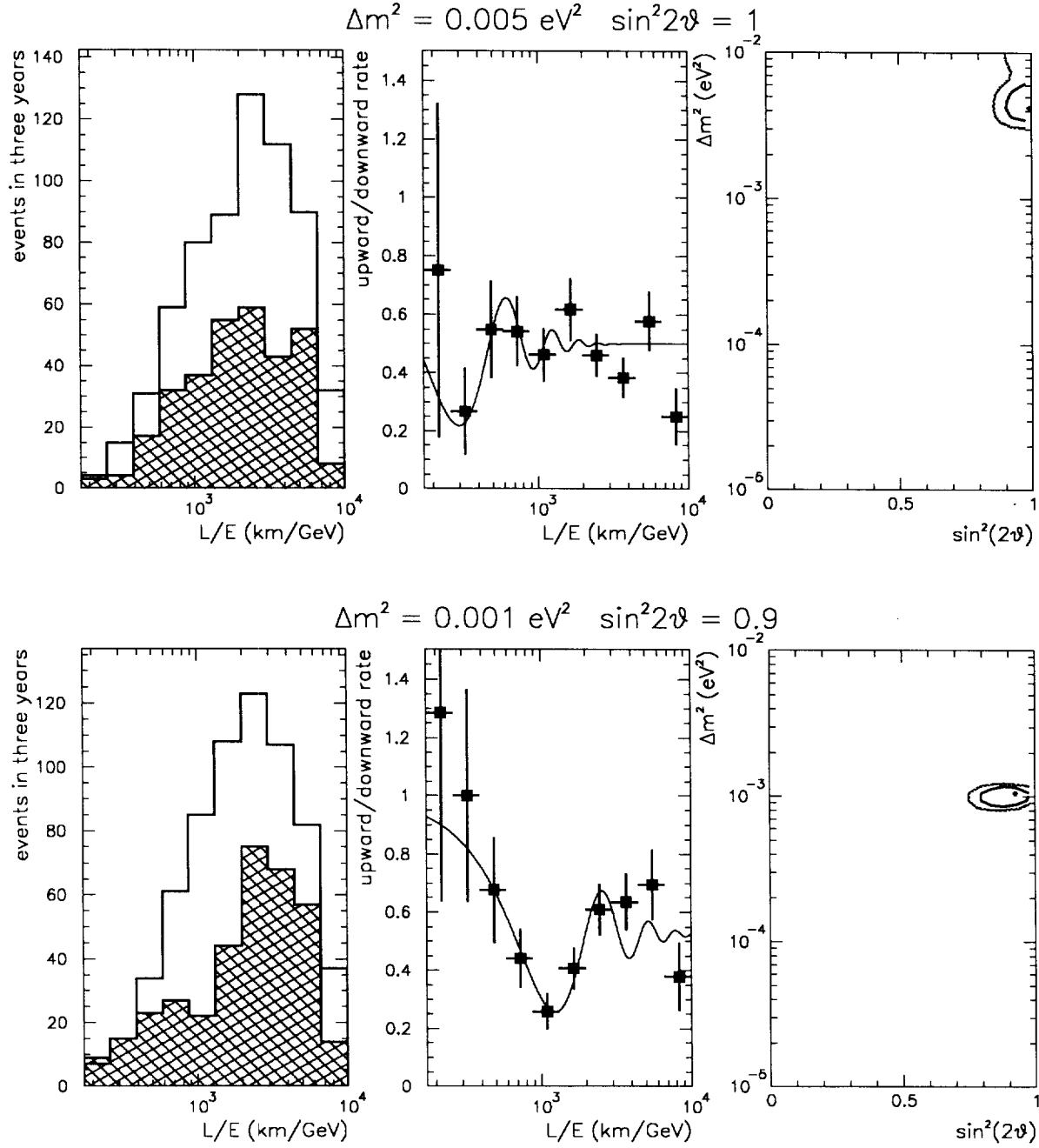


Figure 3: Results of the  $L/E$  analysis on a simulated sample corresponding to three years of data taking in presence of  $\nu_\mu \rightarrow \nu_x$  oscillations, with parameters  $\Delta m^2 = 5 \times 10^{-3} \text{ eV}^2$  and  $\sin^2(2\Theta) = 1.0$  (top) and  $\Delta m^2 = 10^{-3} \text{ eV}^2$  and  $\sin^2(2\Theta) = 0.9$ . The figures show from left to right:  $L/E$  spectra for upward muon events (hatched area) and downward ones (open area); their ratio with the best-fit superimposed and the result of the fit with the corresponding allowed regions for oscillation parameters at 90% and 99% C.L.

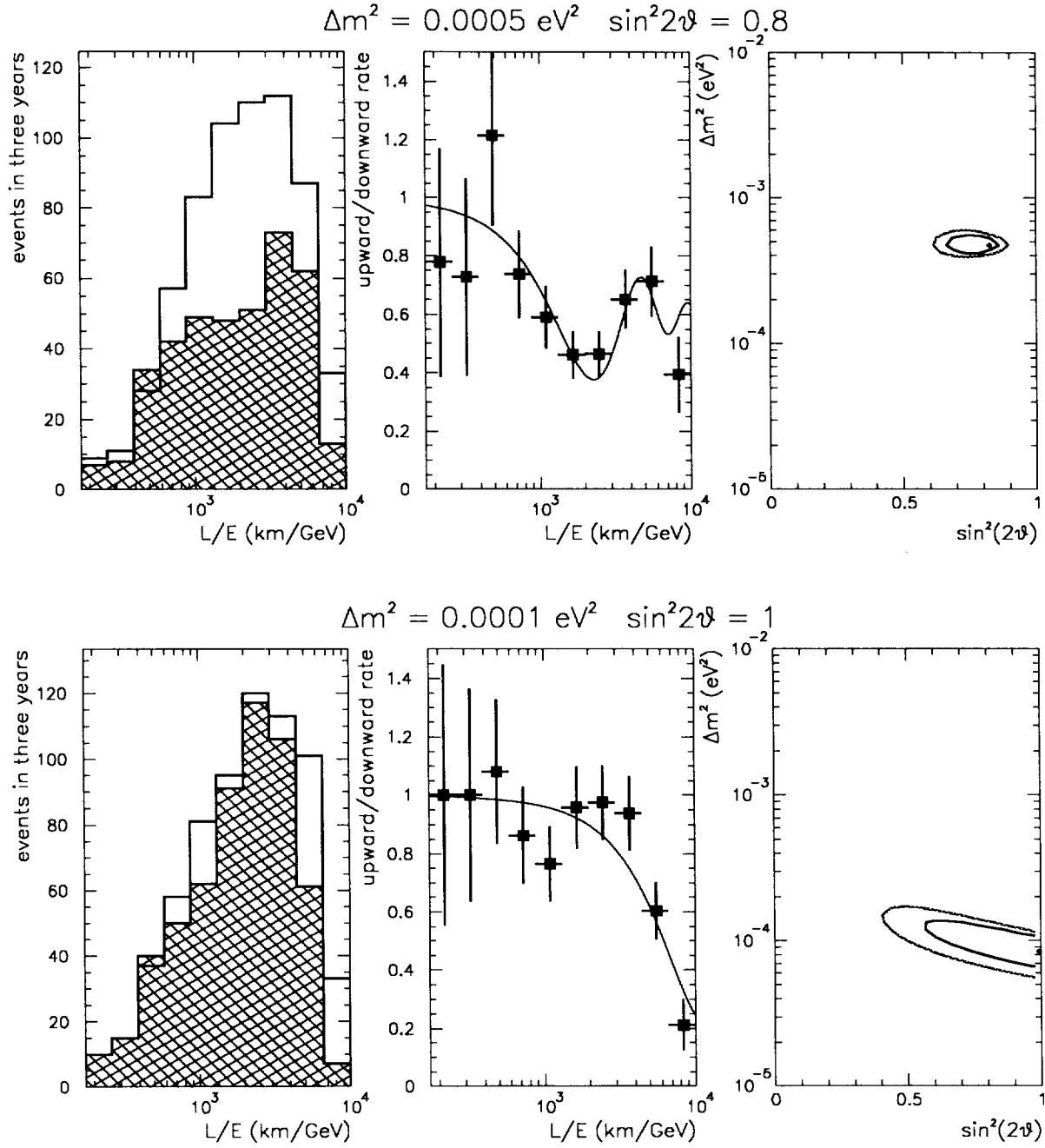


Figure 4: As fig. 3, for  $\Delta m^2 = 5 \times 10^{-4} \text{ eV}^2$  and  $\sin^2(2\Theta) = 0.8$  (top) and  $\Delta m^2 = 10^{-4} \text{ eV}^2$  and  $\sin^2(2\Theta) = 1$  (bottom)

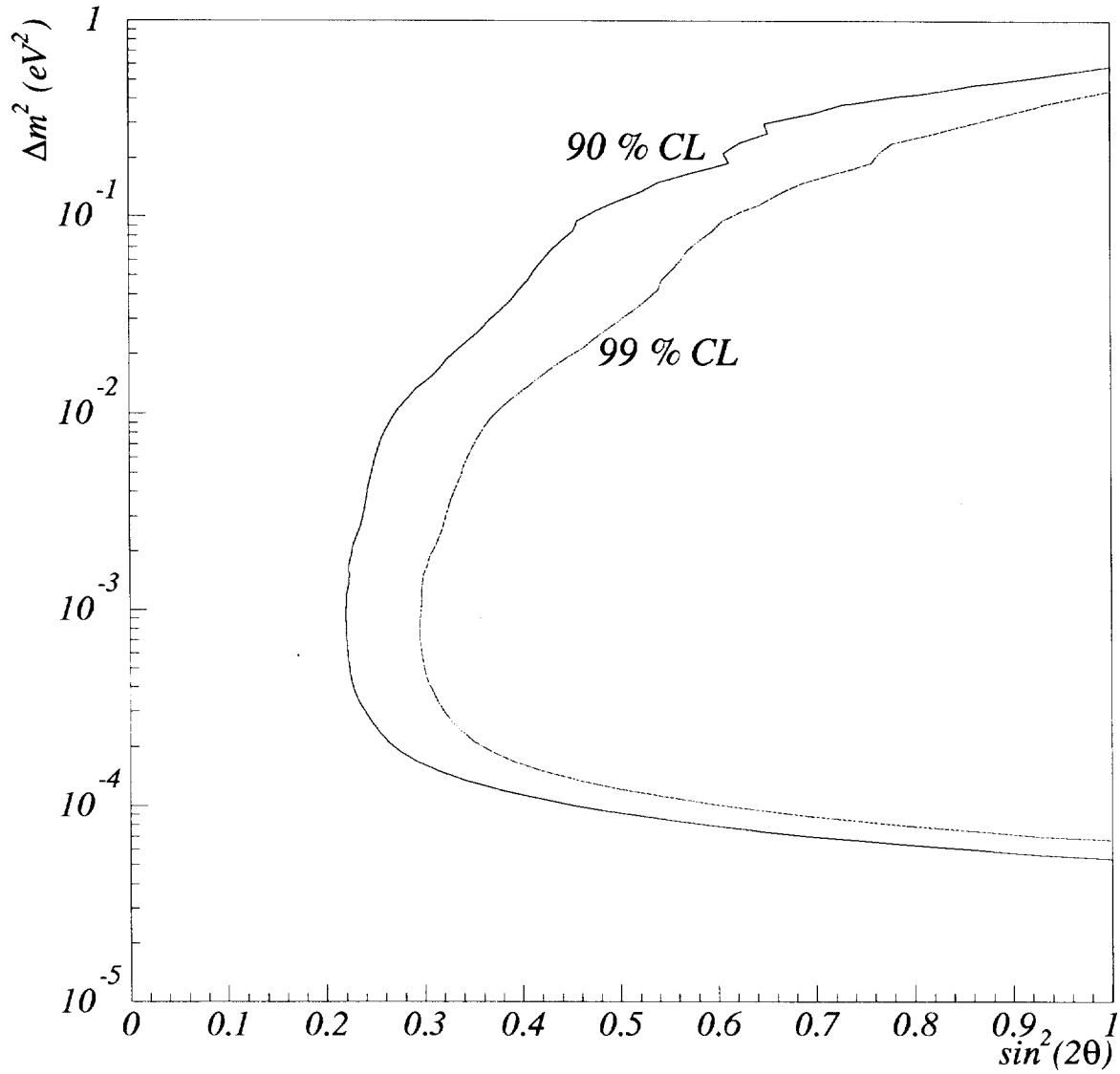


Figure 5: Exclusion curves at 90% and 99% C.L. after three years of data taking assuming no oscillations.

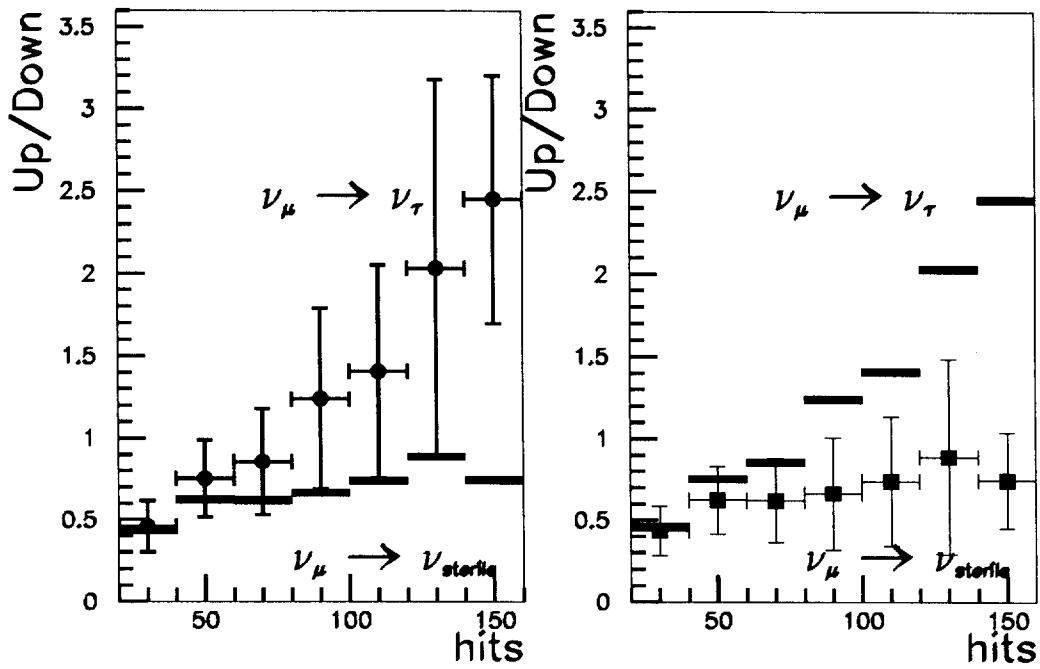


Figure 6: Up/down differential ratios of muon-less events as a function of the number of hits, for  $\Delta m^2 = 5 \times 10^{-3} \text{ eV}^2$  and maximal mixing. The result of the simulation for  $\nu_\mu \rightarrow \nu_\tau$  is compared to the expectations for  $\nu_\mu \rightarrow \nu_{sterile}$  oscillations (left) and vice versa (right). Events have been generated with high statistics, error bars correspond to three years of data taking. The rightmost bin also integrates the contribution of events with hit multiplicity larger than 160.

